Proceedings of the
Annual Stability Conference
Structural Stability Research Council
Charlotte, North Carolina, April 11-14, 2023

Probing the buckling of axially compressed thin stiffened cylindrical shells: Stability landscape and nondestructive prediction

Kshitij Kumar Yadav[1], Simos Gerasimidis[2]

Abstract

Thin shells are highly sensitive to geometric imperfections, and the presence of imperfections reduces their load carrying capacities significantly. Consequently, thin stiffened cylindrical shells are designed conservatively based on the knockdown factor approach that accommodates the uncertainties associated with the underlying imperfections. Recent studies show that methods based on the stability landscape of thin cylinders obtained by probing axially compressed shells in the radially inward direction can predict the capacity of thin shells without measuring the underline imperfections. So far, however, these methods are applied only to thin cylindrical shells without stiffeners. Many outstanding issues must be resolved before applying these methods on thin stiffened cylindrical shells, e.g., the role of stiffeners, the interaction among stiffeners, probing location and imperfections, and the identification of the probing location that yields an accurate capacity prediction. In this study, a stability landscape-based nondestructive procedure is developed for the capacity prediction of imperfect stiffened cylindrical shells by resolving the outstanding issues. Overall, this study reveals three important aspects of the stability landscape-based nondestructive prediction procedure for stiffened cylinders: 1) probing can be used to predict the capacity of imperfect stiffened cylindrical shells without measuring the imperfections, and 2) the probing location plays a crucial role in the accuracy of the prediction, and 3) stability landscape of stiffened cylindrical shells is significantly different than that of unstiffened cylindrical shells.

1. Introduction

The search for high-fidelity estimates of the buckling capacity of thin shells, particularly of cylindrical and spherical thin shells, has long been a cherished goal of the mechanics' community. Thin shells are highly sensitive to imperfections (Koiter 1945), and thus their buckling capacity depends on the shape and the size of each imperfection, as well as their topological arrangement. As a result, we need prior information about the imperfections to make accurate buckling capacity predictions. Information about the shell's underlying imperfections is usually unknown and thus their buckling capacity. Due to the lack of an inexpensive high-fidelity prediction method, thin shells are designed by the conservative knockdown factor

[1] Assistant Professor, Indian Institute of Technology (BHU), Varanasi <kshitij.civ@iitbhu.ac.in >
[2] Assistant Professor, University of Massachusetts, Amherst, <sgerasimidis@umass.edu >

method, which is an empirical method developed by NASA (NASA, 1965) in the late sixties after extensive experimental programs. Using the conservative knockdown factor method, we can design thin shells safely; however, the full engineering potential of thin shells is not being exploited.

Recently, a promising new framework based on the probing of axially compressed shells has emerged for the prediction of the buckling capacity of thin shells without complete knowledge of the shell's underlying imperfections (Thompson 2015, Thompson et al. 2016, Thompson et al. 2017, Hutchinson et al. 2017, Marthelot et al. 2017, Virot et al. 2017, Hutchinson et al. 2018, Fan 2019, Abramian et al. 2020, Yadav et al. 2021, Nicholas et al. 2021). Yadav et al. (2021) have suggested a non-destructive procedure for the evaluation of thin cylindrical shells' axial buckling capacity based on the stability landscape. This procedure consists of three steps: 1) shells are put under axial compression F_a, 2) these axially compressed shells are probed in the radial direction at the location of a pre-existing imperfection, and 3) the peak probe force F_p^{max} and the corresponding axial compression F_a are recorded and used to predict the buckling axial capacity. Ankalhope and Jose (2021) have proposed that the right location for the probing is the least resistant path, and that location can be found by probing at multiple locations. Further, Cuccia et al. (2023) have proposed the right location of probing for the accurate predictions.

All the mentioned studies in the previous paragraph dealt with thin shells without stiffeners, and thus cannot be extrapolated to thin shells with stiffeners. In almost all engineering applications, thin shells are used with stiffeners, and it demands a separate study to evaluate the viability of probing-based prediction methods for thin shells with stiffeners. In this study, we computationally (FEM) investigated the stability landscape of thin stiffened cylindrical shells. First, the buckling of a stiffened cylinder is discussed and compared with the unstiffened cylinder. After that, the probing response of the stiffened cylinder is examined. Finally, the paper is concluded by noticing the main findings of this study.

2. Description of the geometry and finite element model

For this study, a stiffened cylinder is analyzed computationally using the FEA package ABAQUS. The cylinder represents a mini Coke Can (*7.5* fl oz), made of aluminum. The mini Coke Can is modified to make them stiffened along the axial direction. Further, we simplified our modeling assuming the cross-sections of cans are circular throughout the length. The dimensions and material properties of the cylinder are given in Table 1. A total *of 16* stiffeners along the axial directions are attached to the cylinder. The depth *d is 10t* and the width *b is 5t* of the stiffeners, where *t* is the thickness of the cylinder:

Table 1: Dimensions and the material properties of the can

R (*mm*)	*L* (*mm*)	*R/t*	*E* (*Gpa*)	ν
28.6	*107*	*286*	*68.95*	*0.3*

For the meshing, around *66048* four-node reduced integration shell (*S4R*) elements are created, utilizing four integration points along the thickness of each element. Fig. 1 demonstrates the Finite Element Modeling and boundary conditions. For compressing the cylinder to a prescribed axial compression, two nodes are defined at the center of the top and bottom cross-sections of the

cylinder; we call them center nodes. Rigid links are created to connect the nodes at the end of the cylinder to the respective center nodes to constrain the displacements U_1, U_2, and U_3, and rotations UR_1, UR_2, and UR_3 of the nodes at the end from moving and rotating with respect to the center nodes. Using these constraints one end of the cylinder is clamped by fixing the central node at $Z = 0$. At the other end ($Z = L$) a clamped boundary condition is enforced, but the end of the cylinder is loaded by applying an axial displacement $U_3 = -\Delta$.

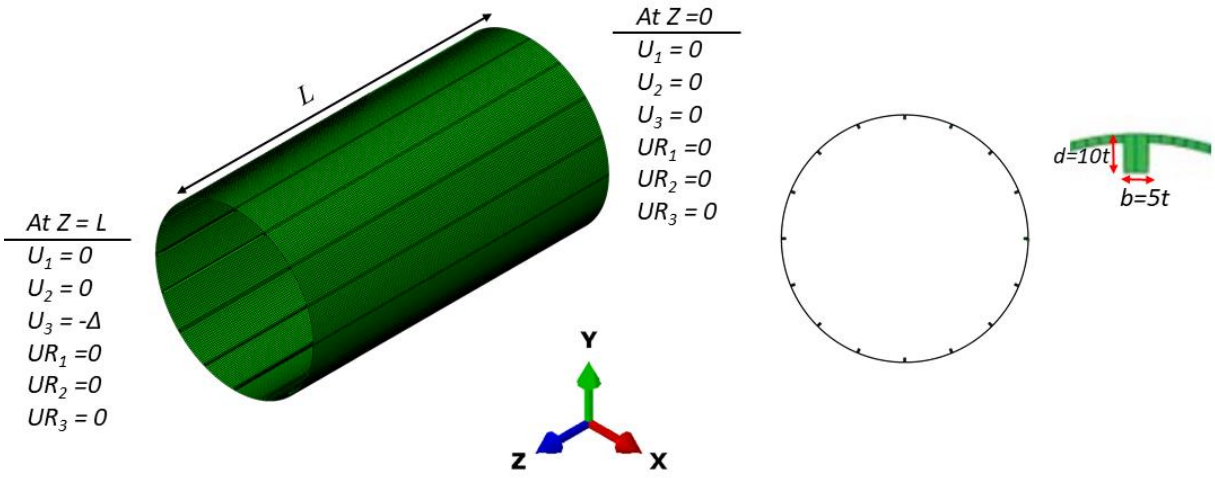

Figure 1: Finite Element Model of the axially stiffened cylinder along with boundary conditions and cross-section of the cylinder. In total 16 stiffeners are used along the axial direction.

3. Result and Discussion

In this section first, we discuss how a perfect axially stiffened cylinder buckled under axial compression. Then, the probing response of the stiffened cylinder is discussed along with the stability landscape.

3.1 Bucking capacity of the perfect stiffened cylinder

The buckling capacity of the perfect stiffened cylinder is found using ABAQUS. The arch-length based Riks method (Riks 1979) is applied for GMNA (Geometric and Material Nonlinear Analysis) to assess the axial strength of the cylinder using S4R elements as described in Section 2. The cylinder is loaded by applying an axial displacement $U3 = -\Delta$ till the cylinder buckled. The cylinder buckled at *3867 N* axial load, and the displacement at the buckling is *0.239544 mm*. The scaled bucked cylinder is shown in Figure 2 (a), and Figure 2 (b) shows the load-displacement plot. The capacity of the stiffened cylinder is substantially more than that of the cylinder without stiffeners. The numerically obtained capacity (using FEA) of the cylinder without stiffeners is *2584.7 N*. Further, the axial displacement of the stiffened cylinder is substantially less than that of the cylinder without stiffeners. These observations are excepted as the stiffeners increase the capacity and stiffness. Figure 3 (a) shows the enlarged view of the stiffeners at the bucking, and Figure 3 (b) shows the scaled deformed shape of the cylinder after buckling. From Figure 3, it is clear that the stiffened cylinder is inheriting the behavior of both the beam and shell. The beam behavior is manifest at the buckling of the cylinder as shown in Figure 3 (a). Once bucking occurred, the stiffeners lose their strength and the shell behavior start manifesting in post-buckling regions as shown in Figure 3 (a). These observations reinforced that

the probing of the unstiffened cylinder cannot be extrapolated to a stiffened cylinder, and a separate study is needed to understand the probing behavior of stiffened cylinder which is the part of next section.

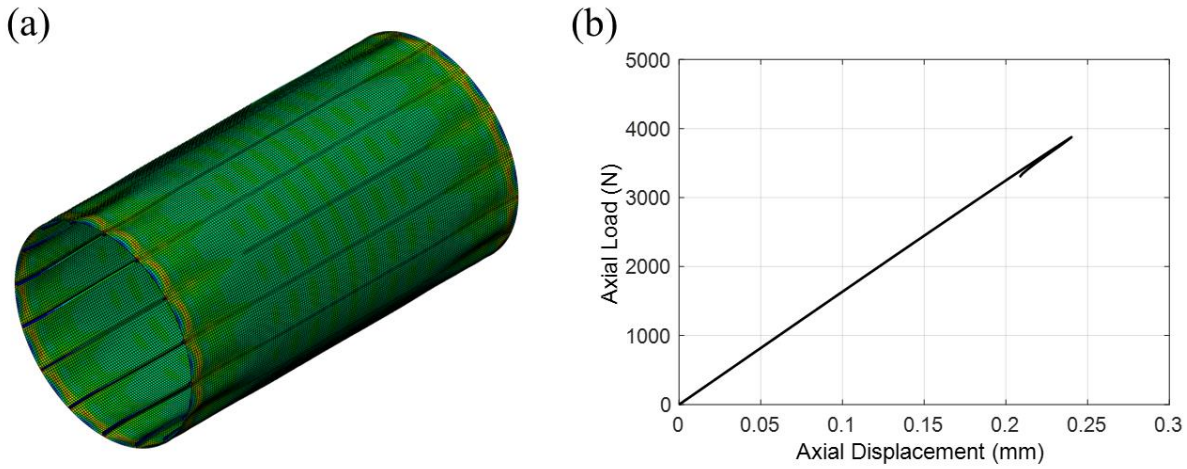

Figure 2: (a) Bucked stiffened cylinder (scaled) under axial compression. The buckling capacity is 3867 N axial load, and the displacement at the buckling is 0.239544 mm. (b) Load-displacement plots of the stiffened cylinder.

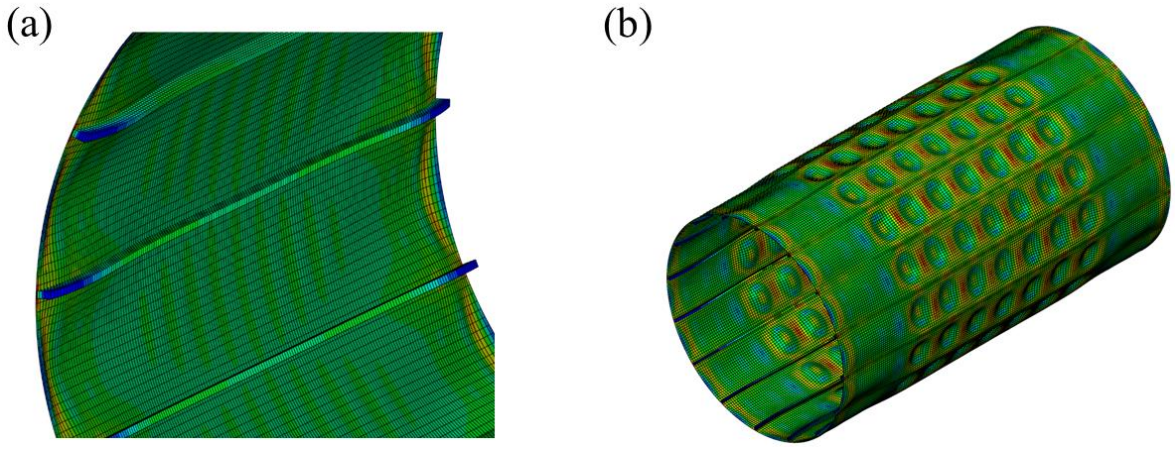

Figure 3: (a) Enlarged view of the stiffeners at the bucking, and (b) scaled deformed shape of the cylinder after buckling.

3.2 Probing and stability landscape of the perfect stiffened cylinder

To evaluate the viability of probing-based prediction methods for stiffened cylindrical shells, we need to understand how stiffened cylindrical shells respond to the probing. For that, we start with the perfect stiffened cylindrical shells. The perfect stiffened cylindrical shell is first compressed under four different axial compressions *2000 N*, *2500 N*, *3300 N*, and *3400 N*, and then probing is done at the middle of the cylinder and the top of a stiffener as shown in Figure 4. Figure 5, shows the response of the compressed stiffened cylindrical shells. Many significant observations can be made from Figure 5. For higher axial compressions, e.g., *Fa = 2500 N, 3300 N,* and *3400N,* the response of probing of the stiffened cylinder is similar to that of an unstiffened perfect cylinder. Initially, the probing force is increasing with probing displacement and reaches a peak, and then reduces as probing displacement is increasing. This is the typical

characteristic of probing unstiffened cylindrical shells. However, for the small axial compression, the response is different than that of the unstiffened cylinder. For small imperfections, initially, the probing force is increasing with probing displacement and reaches a peak, and then the stiffeners buckled as shown in Figure 5 (a). After buckling the stiffener, the cylinder regains strength as shown in Figure 5 (b). This is due to the shell behavior starts playing a role after the buckling of stiffeners. These observations reveal that the probing response of a stiffened cylinder is different and more complex than that of unstiffened cylinders. The complexity comes from the interaction between the stiffeners and the thin shells.

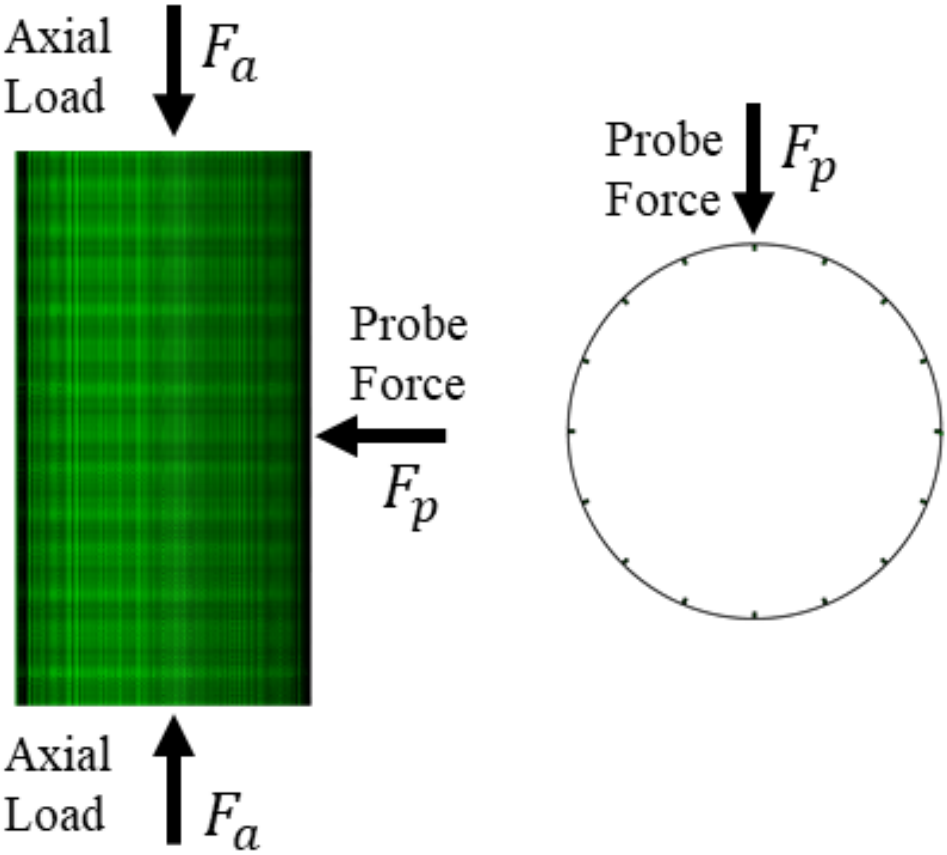

Figure 4: (a) Probing of axially compressed stiffened cylinder. The probing is done at the middle of cylinder and at the top of stiffeners.

4. Conclusions

This study reveals that the probing response of stiffened cylinders is significantly different than previous studies conducted on unstiffened cylinders. The complex interaction between stiffeners and shells is the cause of this difference. As a result, further research is necessary to develop a non-destructive technique for predicting the buckling capacity of stiffened thin cylindrical shells. This study is preliminary and has several limitations, such as only considering perfect stiffened cylinders and only probing at the middle and top of stiffeners. Nevertheless, the results are promising and further studies will be conducted to improve the understanding of the probing response of stiffened cylinders and develop probing-based prediction methods.

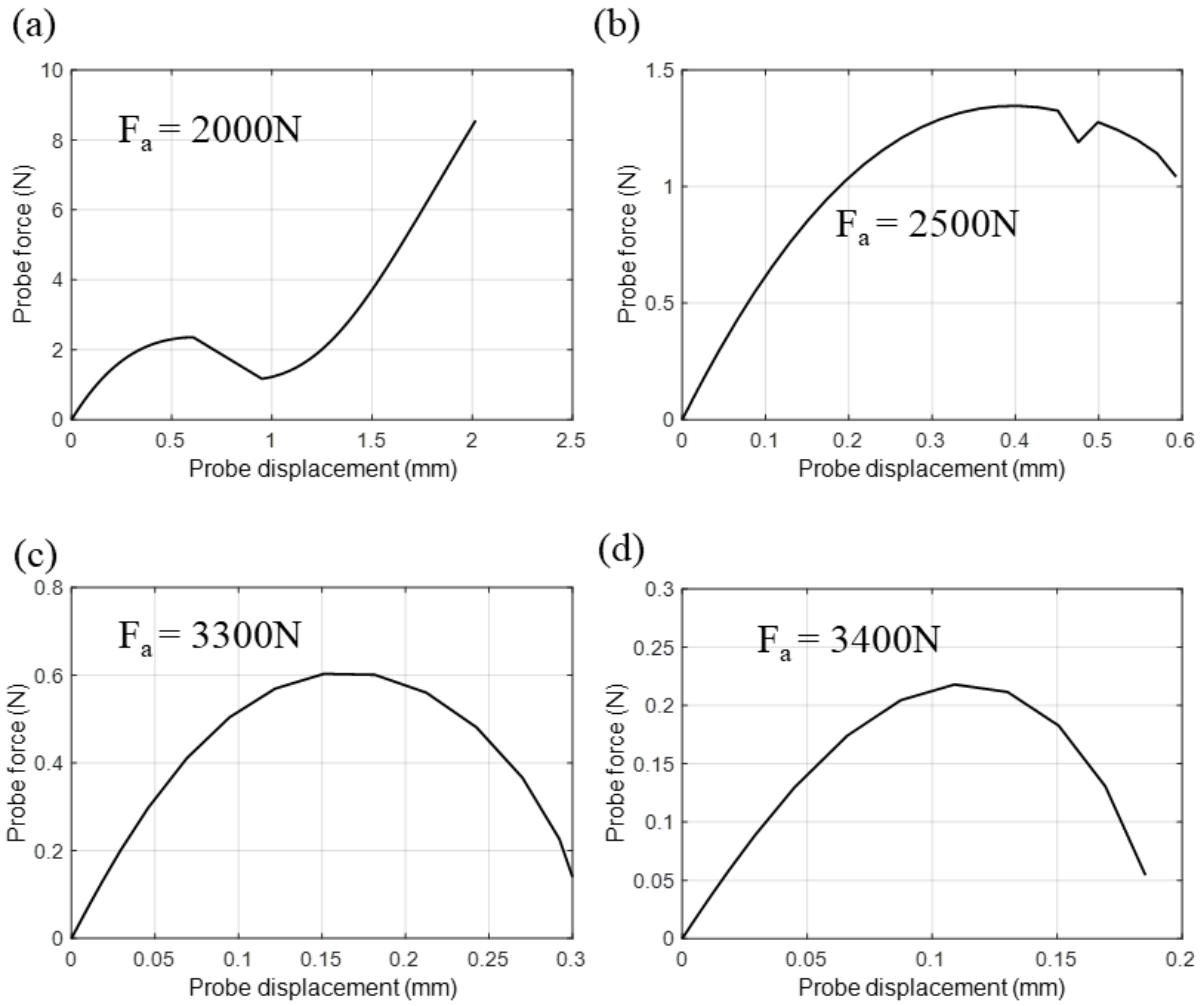

Figure 5: Load-displacement curve of probing of axially compressed stiffened cylinder for axial compression F_a = *2000 N* (a), *2500 N* (b), *3300 N* (c), *3400 N* (d).

References

ABAQUS manual 6.14-14. Dassault Systèmes Simulia Corp.

Abramian A., Virot E., Lozano E., Rubinstein S. M., Schneider T. M., 2020., "Nondestructive prediction of the buckling load of imperfect shells." *Physical Review Letters*, 125 225504.

Ankalhope S, Jose S. "Non-destructive prediction of buckling load of axially compressed cylindrical shells using Least Resistance Path to Probing" *Thin-Walled Structures*, 2022

Cuccia N., Yadav K.K., Virot E., Gerasimidis S., Rubinstein S.M. (2021), "Universal Features of Buckling Initiation in Thin Shells." *Bulletin of the American Physical Society*, 2021.

Cuccia N., Yadav, K.K., Marec Serlin, Virot E., Rubinstein S., & Gerasimidis, S. (2022). Hitting the Mark: Probing at the Initiation Site Allows for Accurate Prediction of a Thin Shell's Buckling Load. *Philosophical Transactions of the Royal Society A*, 2023.

Fan H. (2019), "Critical buckling load prediction of axially compressed cylindrical shell based on non-destructive probing method." *Thin-Walled Structures*, 139 91-104.

Hutchinson J.W., Thompson, J.M.T. (2017), "Nonlinear Buckling Interaction for Spherical Shells Subject to Pressure and Probing Forces*." Journal of Applied Mechanics*, 84 (6) 061001.

Hutchinson J.W., Thompson, J.M.T. (2018), "Imperfections and energy barriers in shell buckling." *International Journal of Solids and Structures*, 148-149 167-168.

Koiter, W. T. (1945). "On the stability of elastic equilibrium." *Thesis Deft, H.J. Paris, Amsterdam*

Marthelot J., Jiménez F.L., Lee A., Hutchinson J.W., Reis P.M. (2017), "Buckling of a Pressurized Hemispherical Shell Subjected to a Probing Force." *Journal of Applied Mechanics*, 84 (12) 121005.

Riks E. (1979), "An incremental approach to the solution of snapping and buckling problems." *International Journal of Solids and Structures*, 15(7) 529-551.

Thompson, J.M.T. (2015), "Advances in Shell Buckling: Theory and Experiments." *International Journal of Bifurcation and Chaos*, 25 (01) 153001.

Thompson, J.M.T., Sieber J. (2016), "Shock-Sensitivity in Shell-Like Structures: With Simulations of Spherical Shell Buckling." *International Journal of Bifurcation and Chaos*, 26 (02) 1630003.

Thompson, J.M.T., Hutchinson J.W., Sieber J. (2017), "Probing Shells Against Buckling: A Nondestructive Technique for Laboratory Testing." *International Journal of Bifurcation and Chaos*, 27 (14) 1730048.

Virot E., Kreilos T., Schneider T.M., Rubinstein S.M. (2021), "Stability Landscape of Shell Buckling." *Physical Review Letters*, 119 224101.

Yadav K.K., Cuccia N., Virot E., Gerasimidis S., Rubinstein S.M. (2021), "A non-destructive technique for the evaluation of thin cylindrical shells' axial buckling capacity." *Journal of Applied Mechanics*, 88(5), 051003.

Yadav K.K., Cuccia N., Virot E., Gerasimidis S., Rubinstein S.M. (2021), "Prediction of the buckling capacity of thin shells by using stability landscapes." *Bulletin of the American Physical Society*.

Yadav, K.K., & Gerasimidis, S. (2020). Imperfection insensitive thin cylindrical shells for next generation wind turbine towers. *Journal of Constructional Steel Research*, 172, 106228.

Yadav, K.K., & Gerasimidis, S (2020). Imperfection Insensitivity of Thin Wavy Cylindrical Shells Under Axial Compression or Bending. *Journal of Applied Mechanics*, 87(4), 041003.

Yadav K.K., Gerasimidis S (2019). "Instability of thin steel cylindrical shells under bending" *Thin-Walled Structures*, 137, 151-166.

Yadav, K.K. , Sloance Z., and Gerasimidis, S (2022). Probing the buckling of axially compressed cylindrical shells: Stability landscape and nondestructive prediction, *Proceedings of the Annual Stability Conference Structural Stability Research Council (SSRC)*, Denver, Colorado, April 21-24.